

CO₂ Conversion: The Potential of Porous–Organic Polymers (POPs) for catalytic CO₂-epoxides insertion

Mohamed H. Alkordi,^{1a‡} Łukasz J. Weseliński,^{1a§} Valerio D’Elia,^{bc} Samir Barman,^b Amandine Cadiau,^a
Mohamed N. Hedhili,^d Amy J. Cairns,^a Rasha Abdulhalim,^a Jean-Marie Basset,^b and Mohamed
Eddaoudi^{a*}

[†]These authors contributed equally

^aFunctional Materials Design, Discovery and Development Research Group (FMD³),
Advanced Membranes and Porous Materials Center, Division of Physical Sciences
and Engineering, King Abdullah University of Science and Technology (KAUST),
Thuwal 23955-6900, Kingdom of Saudi Arabia.

E-mail: mohamed.eddaoudi@kaust.edu.sa

^bKAUST Catalysis Center (KCC), King Abdullah University of Science and Technology (KAUST),
Thuwal 23955-6900, Kingdom of Saudi Arabia.

^cCurrent address: Department of Materials Science and Engineering, Vidyasirimedhi Institute of Science and Technology,
21210, WangChan, Rayong, Thailand.

^dImaging and Characterization Laboratory, King Abdullah University of Science and Technology (KAUST),
Thuwal 23955-6900, Kingdom of Saudi Arabia.

[‡]Current address: Zewail City of Science and Technology, Center for Materials Science, Sheikh Zayed Dist.,
6th of October, 12588, Giza, Egypt.

[§]Current address: Department of Chemistry, Michigan Technological University,
1400 Townsend Drive, Houghton, Michigan 49931, United States.

Table of Contents

Materials and methods.....	2
Synthesis of 1, 1-Co, and 1-Cr:.....	3
Powder X-ray diffraction patterns.....	5
FT-IR spectra	6
TGA analyses.....	7
UV-Vis spectra for 1, 1-Co and 1-Cr.....	8
Nitrogen sorption isotherms for 1 and BET plots for 1, 1-Co and 1-Cr	9
Pore size distribution.....	11
Detailed XPS study of 1-Co and 1-Cr.....	12
Solid-state NMR spectrum for 1	16
Scanning Electron Microscope (SEM) images of 1, 1-Cr and 1-Co.....	17
EDX (Energy-dispersive X-ray spectroscopy) analysis of 1, 1-Cr and 1-Co	18
References.....	21

Materials and methods

All reagents were obtained from commercial vendors and used as received unless further noticed. Liquid NMR spectra were recorded at room temperature with Bruker Avance III 500MHz spectrometer using CDCl_3 as a solvent. Cross polarization magic angle spinning (CP-MAS) solid state ^{13}C NMR spectra were recorded with Bruker Avance 600 WB spectrometer. Elemental analysis was performed with a Thermo Scientific Flash 2000 instrument. Powder X-ray Diffraction (PXRD) measurements were carried out at room temperature on a PANalytical X'Pert PRO diffractometer 45kV, 40mA for $\text{CuK}\alpha$ ($\lambda = 1.5418 \text{ \AA}$) with a scan speed of $0.02^\circ.\text{min}^{-1}$ and a step size of 0.008° in 2θ . UV spectra were recorded with a Perkin Elmer Lambda 950 UV/VIS spectrometer. Thermogravimetric analysis (TGA) measurements were performed on a TA Q500 apparatus, under air atmosphere (flow = $25 \text{ cm}^3.\text{min}^{-1}$, heating rate $5^\circ\text{C}.\text{min}^{-1}$). Fourier-transform Infrared (FT-IR) spectra ($4000 - 600 \text{ cm}^{-1}$) were recorded on a Thermo Scientific Nicolet 6700 apparatus. Low-pressure gas sorption measurements were performed on a fully automated Autosorb 6B (for N_2 sorption screening) and Autosorb-iQ gas adsorption analyzer (Quantachrome Instruments) at relative pressures up to 1 atm. The cryogenic temperatures were controlled using liquid nitrogen and argon baths at 77 K and 87 K, respectively. Pore size distributions were calculated using QSDFT pore size analysis method for carbons with slit-shaped/cylindrical/spherical pores. ICP-OES measurements of the metal loading on the porous materials were carried out on a Varian 720-ES instrument after digestion of a 10 mg sample in *aqua regia*. XPS studies were carried out in a Kratos Axis Ultra DLD spectrometer equipped with a monochromatic Al $\text{K}\alpha$ x-ray source ($h\nu=1486.6 \text{ eV}$) operating at 150 W, a multichannel plate and delay line detector under a vacuum of $1\sim 10^{-9}$ mbar. The survey and high-resolution spectra were collected at fixed analyzer pass energies of 160 eV and 20 eV, respectively. Samples were mounted in floating mode in order to avoid differential charging. Charge neutralization was required for all samples. Binding energies were referenced to the aromatic sp^2 hybridized ($\text{C}=\text{C}$) carbon for the C 1s peak set at 284.5 eV. The morphology of samples was determined by field-emission scanning electron microscope (FESEM, FEI Nova Nano 630). The chemical compositions of samples were analyzed by energy dispersive spectrometer (EDX, Quanta 600).

Synthesis of **1**, **1-Co**, and **1-Cr**:

(1) Synthesis of *N,N'*-bis(5-bromosalicylaldehyde)cyclohexanediimine: a reported procedure was followed.¹A suspension of *trans*-cyclohexane-1,2-diamine (1.71 g, 15 mmol) and 5-bromo-2-hydroxybenzaldehyde (6.03 g, 30 mmol) in absolute ethanol (20 ml) was vigorously stirred at 75 °C under Ar for 14 h. It was cooled, filtered on paper, thoroughly washed with ethanol and dried on air to produce yellow solid, 6.56 g (97%). ¹H NMR (500MHz, CDCl₃): δ = 13.3 (s, 2H), 8.18 (s, 2H), 7.33 (dd, *J* = 2.4, 8.8 Hz, 2 H), 7.26 (s, 2 H), 6.80 (d, *J* = 8.8 Hz, 2 H), 3.33 (m, 2 H), 1.90 (m, 4 H), 1.74 (m, 2H), 1.47 (m, *J* = 9.9 Hz, 2 H). ¹³C NMR (126MHz, CDCl₃): δ = 163.6, 160.1, 135.1, 133.7, 120.0, 119.0, 110.3, 72.8, 33.0, 24.2.

(2) Synthesis of **1**: the material was synthesized following the reported procedure.²In a 150 ml oven-dried round bottom flask, a solution of *N,N'*-bis(5-bromosalicylaldehyde)cyclohexanediimine (0.96 g, 2 mmol) in dry DMF (30 ml, stored over CaH₂) and dry triethylamine (6 ml) was bubbled with Ar for 30 min. Then, 1,3,5-triethynylbenzene (0.3 g, 2 mmol), PdCl₂(PPh₃)₂ (44 mg, 0.063 mmol), and CuI (12 mg, 0.063 mmol) were added in one portion, the solution was evacuated/backfilled with Ar 3 times, sealed with septum and heated at 80 °C for 50 h with vigorous stirring. It was cooled, filtered, solid washed sequentially with DMF, water, THF, MeOH and acetone, then suspended in 1/1THF/CH₂Cl₂(80 ml), and stirred at rt for 48 h, refreshing solution twice daily. It was filtered, washed with THF and dried at high vacuum at 60 °C overnight to give red-brown solid, 0.57 g. Calc. for C₈₄H₆₆N₆O₆: C, 80.36; H, 5.30; N, 6.69; O, 7.65. Found C, 79.8; H, 4.58; N, 4.16.

(3) Synthesis of **1-Co**. In a 150 ml oven-dried round bottom flask, a solution of *N,N'*-bis(5-bromosalicylaldehyde)cyclohexanediimine (0.96 g, 2 mmol) and CoBr₂ (0.438 g, 2 mmol) in dry DMF (30 ml, stored over CaH₂) was heated at 110 °C under Ar for 30 min. It was cooled to rt to afford deep green solution. To the solution of metalated salene ligand, dry triethylamine (6 ml) was added causing change of color to deep red. The flask was evacuated/backfilled with Ar twice, and the mixture bubbled with Ar for 30 min. Then, 1,3,5-triethynylbenzene (0.3 g, 2 mmol), PdCl₂(PPh₃)₂ (44 mg, 0.063 mmol), and CuI (12 mg, 0.063 mmol) were added in one portion, the flask was evacuated/backfilled with Ar three times, sealed with septum and heated at 80 °C for 48 h with vigorous stirring. It was cooled, filtered, solid washed sequentially with DMF, water, THF, MeOH and acetone, then suspended in 1/1/1 CH₂Cl₂/H₂O/MeOH/acetone(160 ml), and stirred at 80 °C for 20 h. It was filtered, washed with acetone and dried at high vacuum at 60 °C overnight to give dark red solid, 1.35 g. Calc. for C₈₄H₆₀N₆O₆Co₃Br₃: C, 60.56; H, 3.63; Br, 14.39; Co, 10.61; N, 5.04; O, 5.76. Found C, 55.58; H, 3.48; N, 4.00.

(4) Synthesis of **1-Cr**. In a 150 ml oven-dried round bottom flask, a solution of *N,N'*-bis(5-bromosalicylaldehyde)cyclohexanediiimine (0.96 g, 2 mmol) and CrCl_2 (0.246 g, 2 mmol) in dry DMF (30 ml, stored over CaH_2) was heated at 110 °C under Ar for 30 min. It was cooled to rt to afford dark brown solution. To the solution of metalated salene ligand, dry triethylamine (6 ml) was added, the flask was evacuated/backfilled with Ar twice, and the mixture bubbled with Ar for 30 min. Then, 1,3,5-triethynylbenzene (0.3 g, 2 mmol), $\text{PdCl}_2(\text{PPh}_3)_2$ (44 mg, 0.063 mmol), and CuI (12 mg, 0.063 mmol) were added in one portion and the same synthetic procedure and work-up as for **1-Co** was followed to give green brown solid, 0.6 g. Calc. for $\text{C}_{84}\text{H}_{60}\text{N}_6\text{O}_6\text{Cr}_3\text{Cl}_3$: C, 66.74; H, 4.00; Cl, 7.04; Cr, 10.32; N, 5.56; O, 6.35. Found C, 68.16; H, 3.90; N, 2.44.

Powder X-ray diffraction patterns

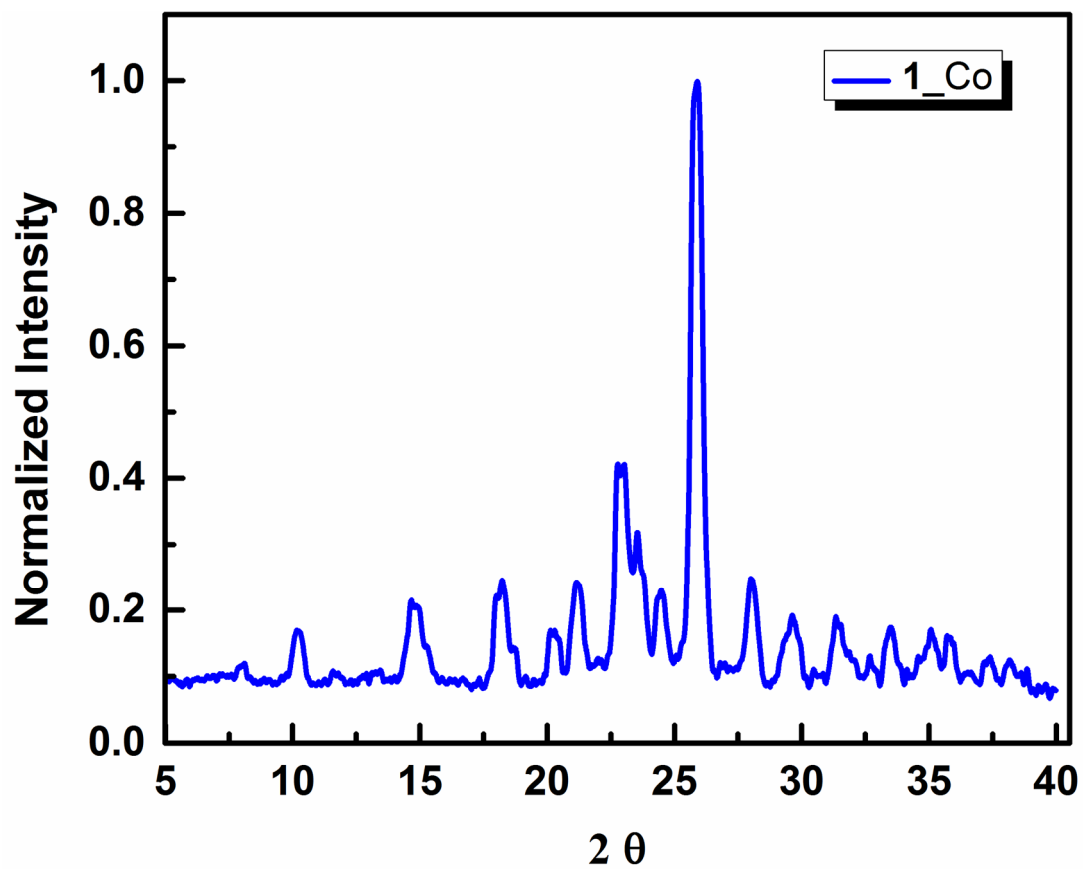


Figure S1. PXRD patterns for 1-Co.

FT-IR spectra

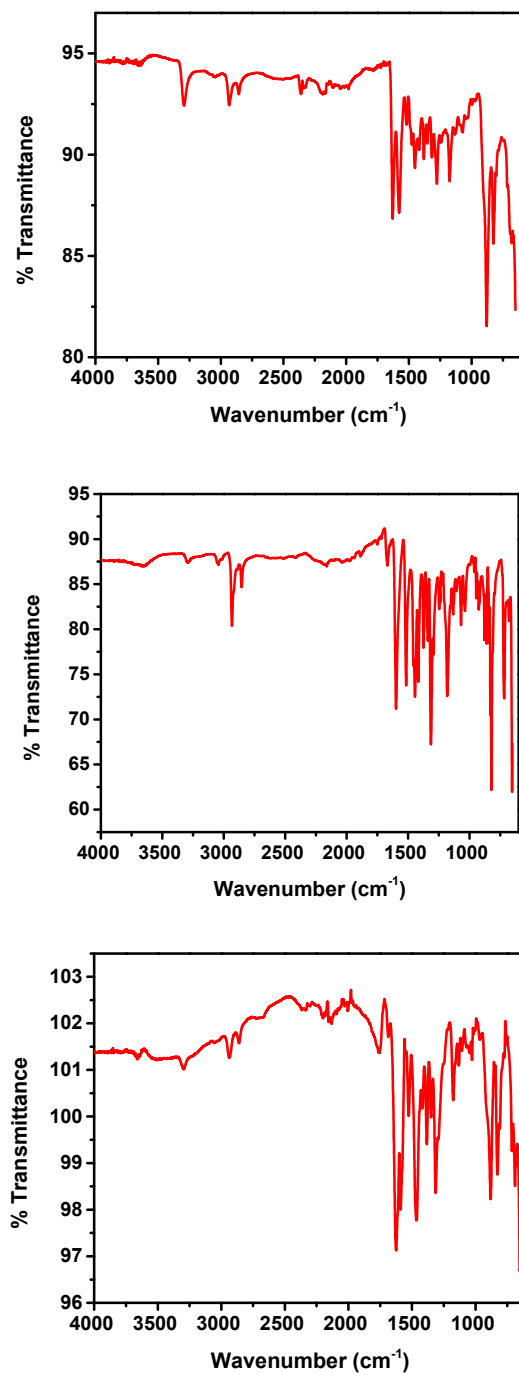


Figure S2. FT-IR spectra for **1** (above), **1-Co** (middle), and **1-Cr** (bottom). The free phenolic O–H stretch frequency in the non-metated POP (3294 cm⁻¹) is absent or significantly reduced in the metalated salen POPs **1-Co** and **1-Cr**.

TGA analyses

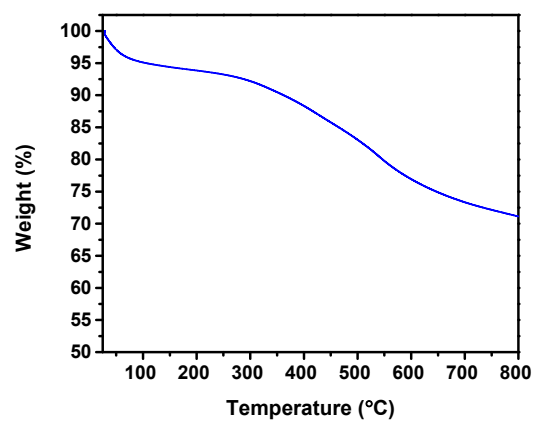
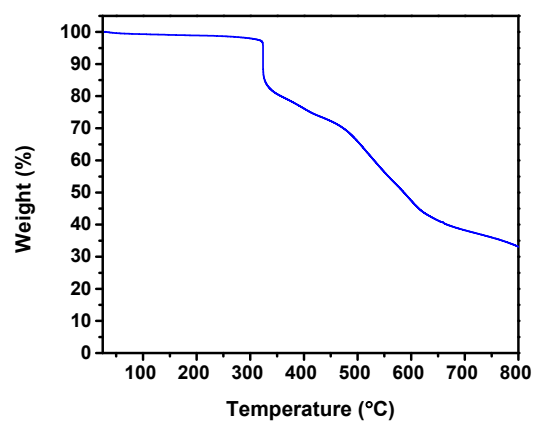
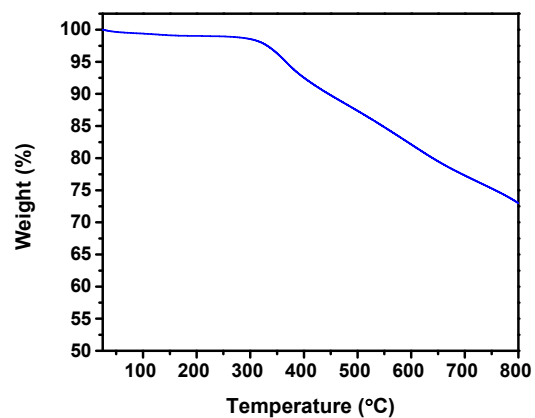


Figure S3. Thermogravimetric analyses of **1** (top), **1-Co** (middle) and **1-Cr** (bottom).

UV-Vis spectra for 1, 1-Co and 1-Cr

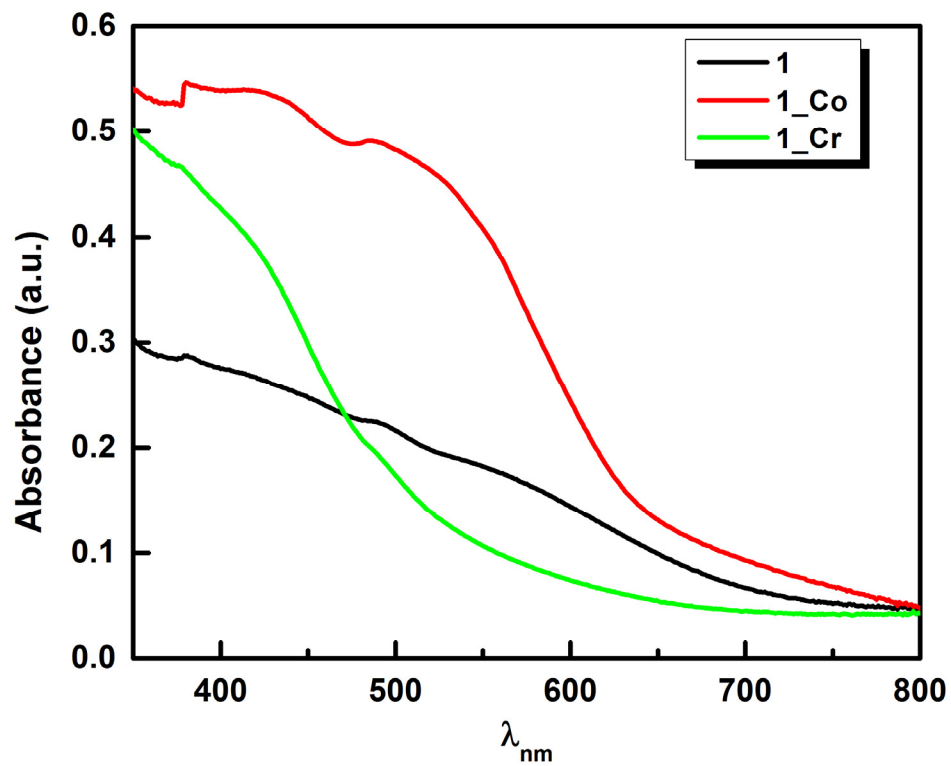
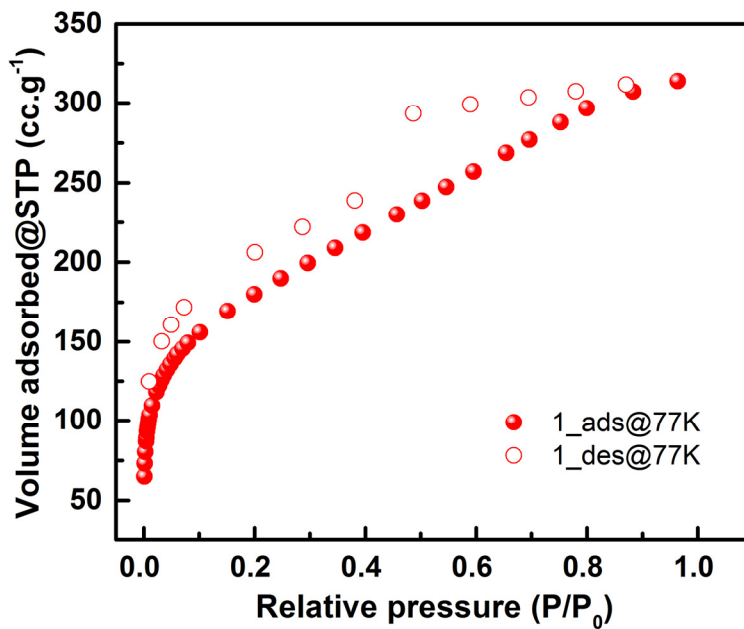
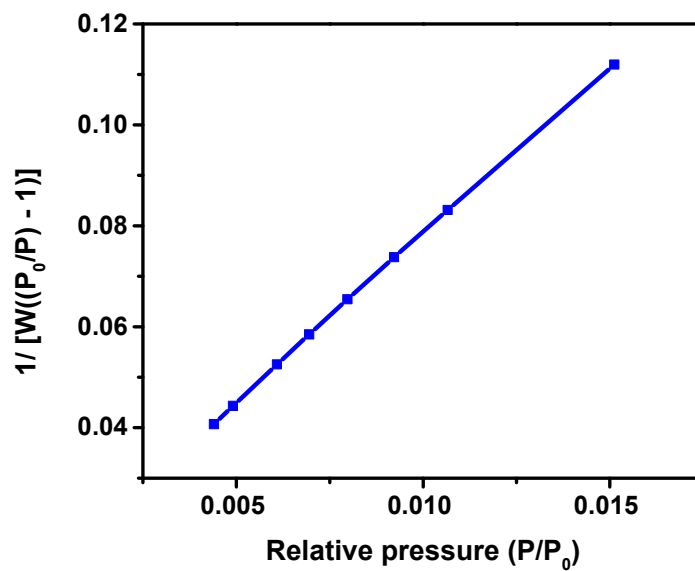


Figure S4. UV-Vis diffuse absorption spectra for 1 (black), 1-Co (red) and 1-Cr (green)

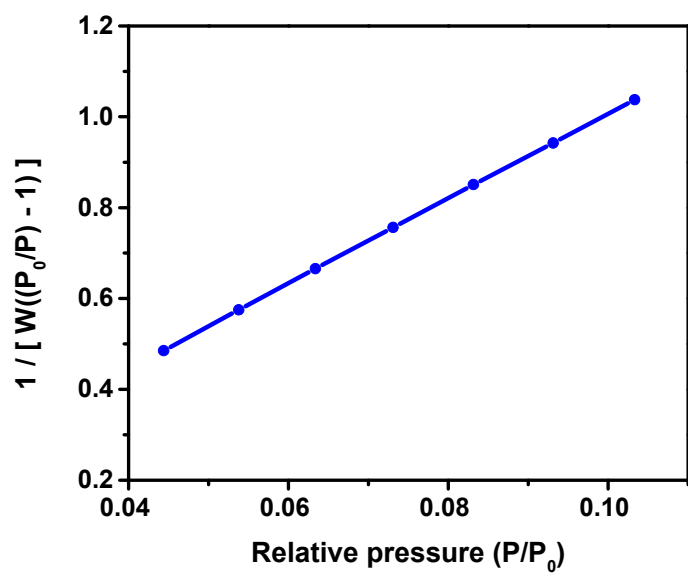
Nitrogen sorption isotherms for 1 and BET plots for 1, 1-Co and 1-Cr



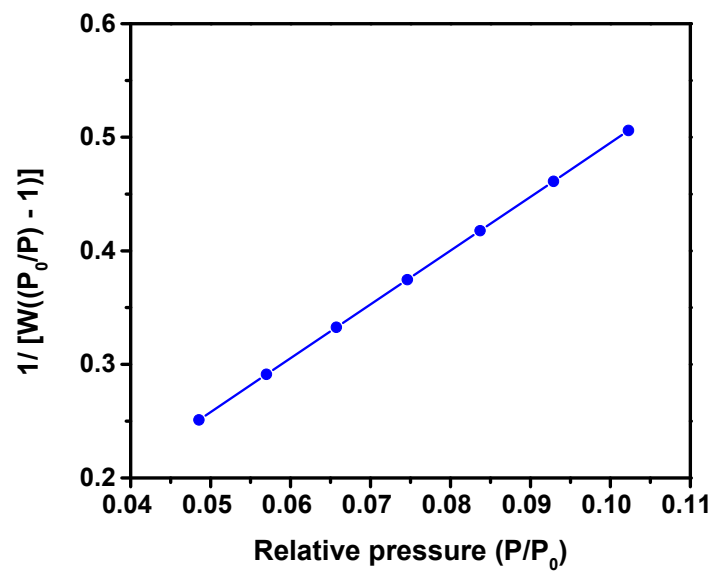
BET surface area: 523 m²/g



BET plot for 1



BET plot for 1-Co



BET plot for 1-Cr

Figure S5. N₂ sorption isotherms for 1, BET plots for 1, 1-Co, and 1-Cr.

Pore size distribution

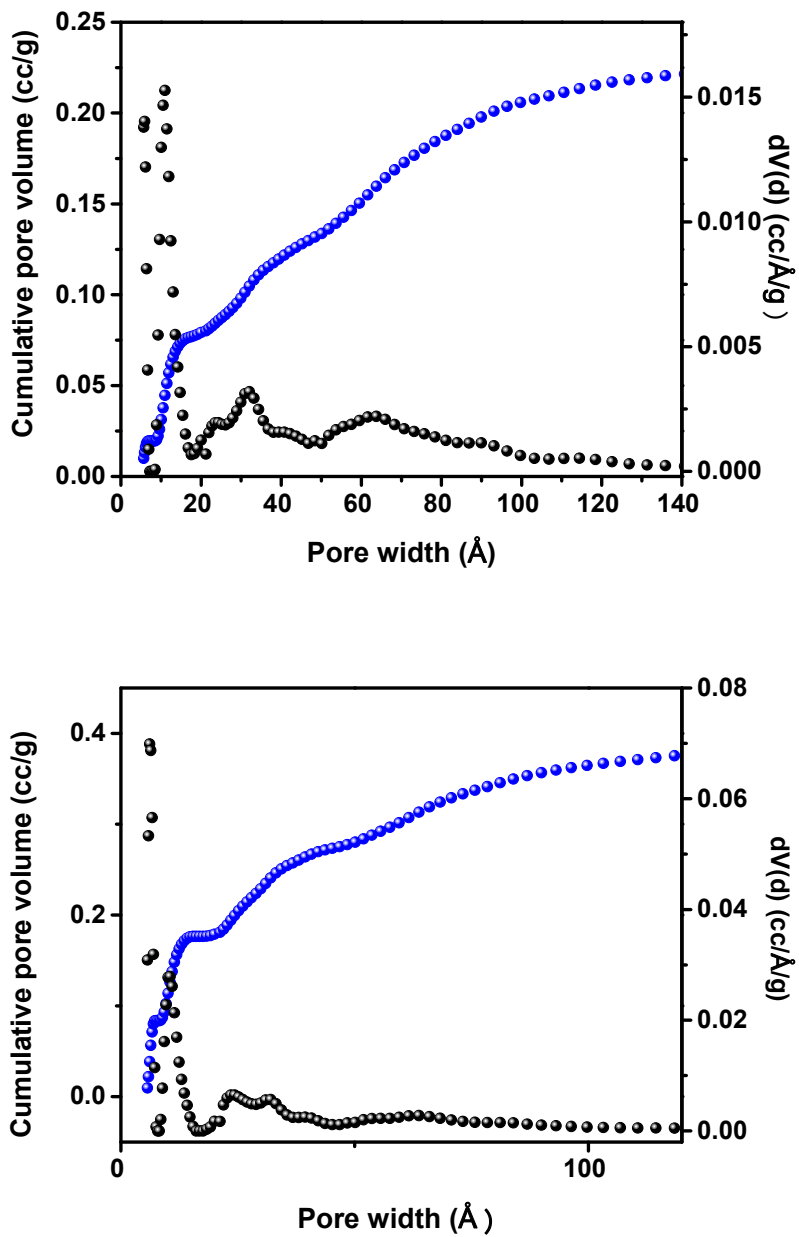


Figure S6. Pore size distribution for 1-Co (top) and 1-Cr (bottom).

Detailed XPS study of 1-Co and 1-Cr

XPS investigations were performed to characterize the chemical composition of the surface of the powdered samples and to determine the oxidation state of cobalt and chromium for **1-Co** and **1-Cr**.

The survey spectrum of **1-Cr** shows that Cr, O, C, N, Cl, and Br elements are detected (Figure S7).

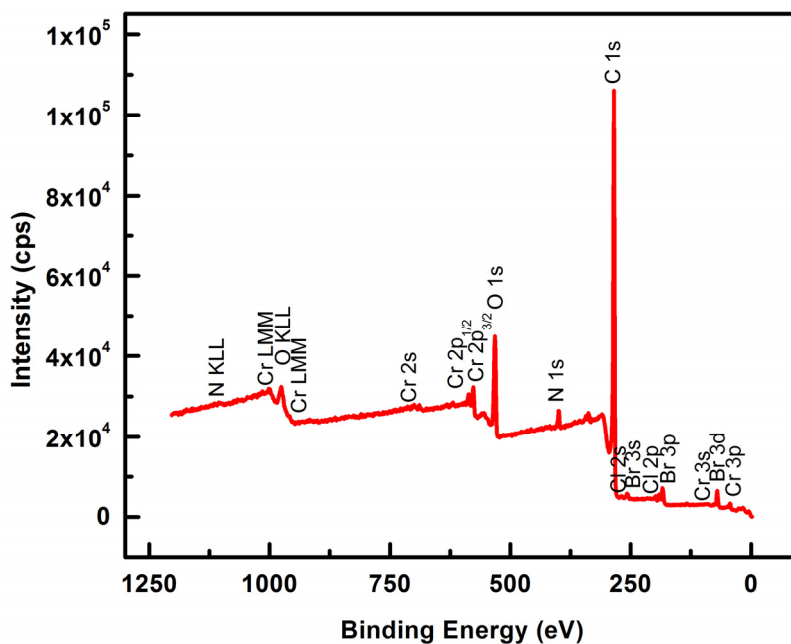


Figure S7. Survey XPS spectrum of **1-Cr**.

High resolution XPS spectrum of Cr 2p core level was obtained from **1-Cr** powdered sample (Figure S8). The Cr 2p region shows one doublet situated at 576.6 eV and 586.4 eV corresponding to Cr 2p_{3/2} and Cr 2p_{1/2} spin-orbit split components respectively. Additionally, a satellite structure is observed at 597.6 eV corresponding to a shake-up satellite for Cr 2p_{1/2} component. The satellite peak of Cr 2p_{3/2} component strongly overlaps with Cr 2p_{1/2} peak. The binding energies of the components of Cr 2p doublet and their corresponding satellites are characteristic for Cr³⁺ oxidation state of chromium.³

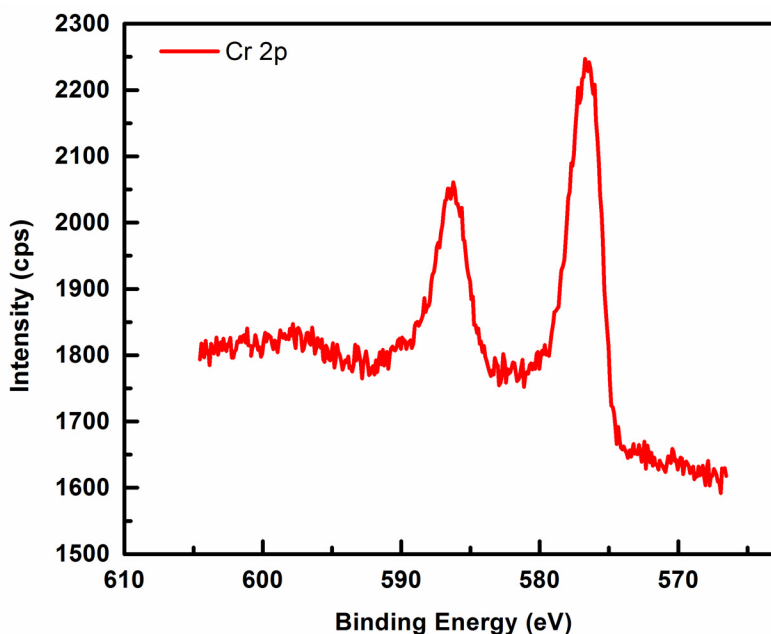


Figure S8. High resolution XPS spectrum of Cr 2p core level for **1-Cr**

The survey spectrum of **1-Co** shows that Cr, O, C, N, and Br elements are detected (Figure S9).

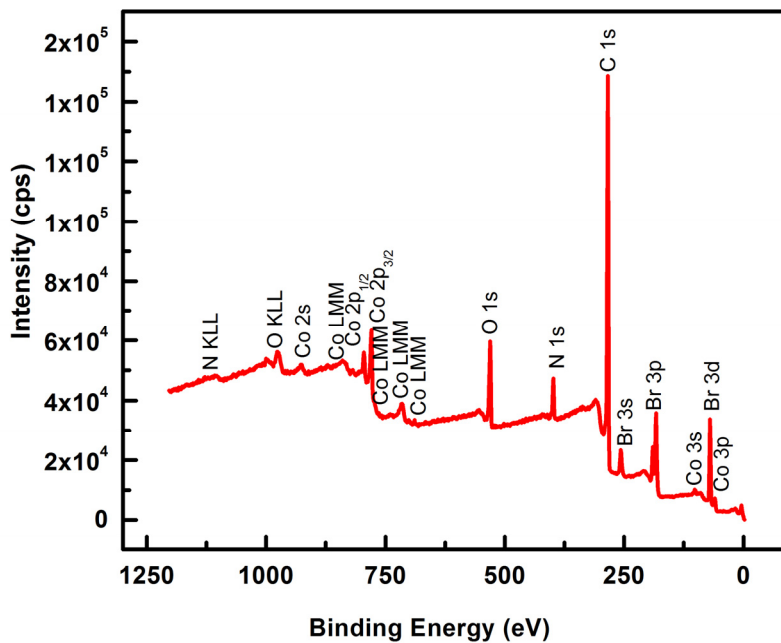


Figure S9. Survey XPS spectrum of **1-Co**.

High resolution XPS spectrum of Co 2p core level was obtained from **1-Co** powdered sample (Figure S10). The Co 2p region shows one doublet situated at 779.5 eV and 795.7 eV corresponding to Co 2p_{3/2} and Co 2p_{1/2} spin-orbit split components, respectively.

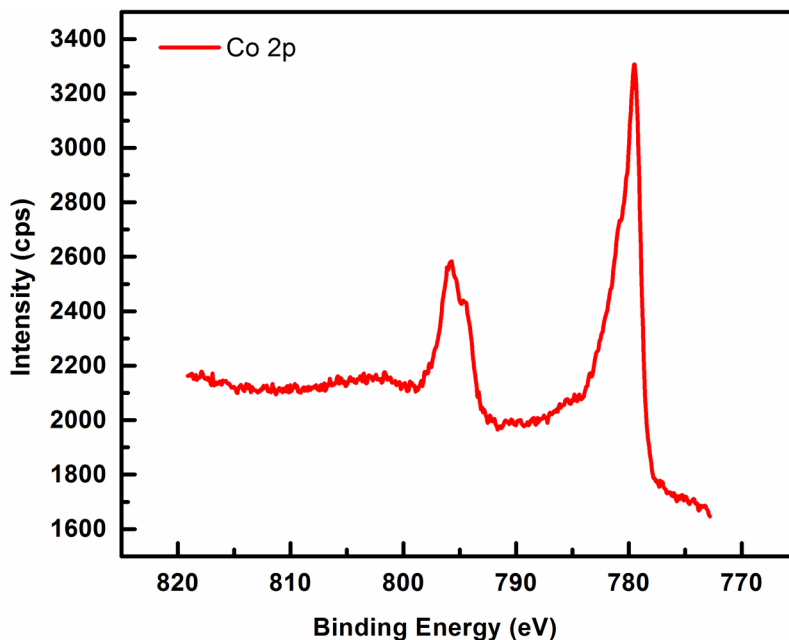


Figure S10. High resolution XPS spectrum of Cr 2p core level for **1-Co**

The binding energies of the components of Co 2p doublet correspond to Co³⁺ oxidation state.⁴ We can notice the presence of a weak 2p satellite features about 10 eV higher from the Co 2p components around ~790 eV and ~805 eV which are characteristic for Co³⁺ cations.⁴

We observe also a shoulder at 780.8 eV for Co 2p_{3/2} component accompanied with satellite peak around ~786 eV associated to the presence of Co²⁺ cations.³ The results indicate that the dominant oxidation of cobalt for **1-Co** powdered sample is 3+ with the presence of traces of additional Co²⁺ cations.

Solid-state NMR spectrum for 1

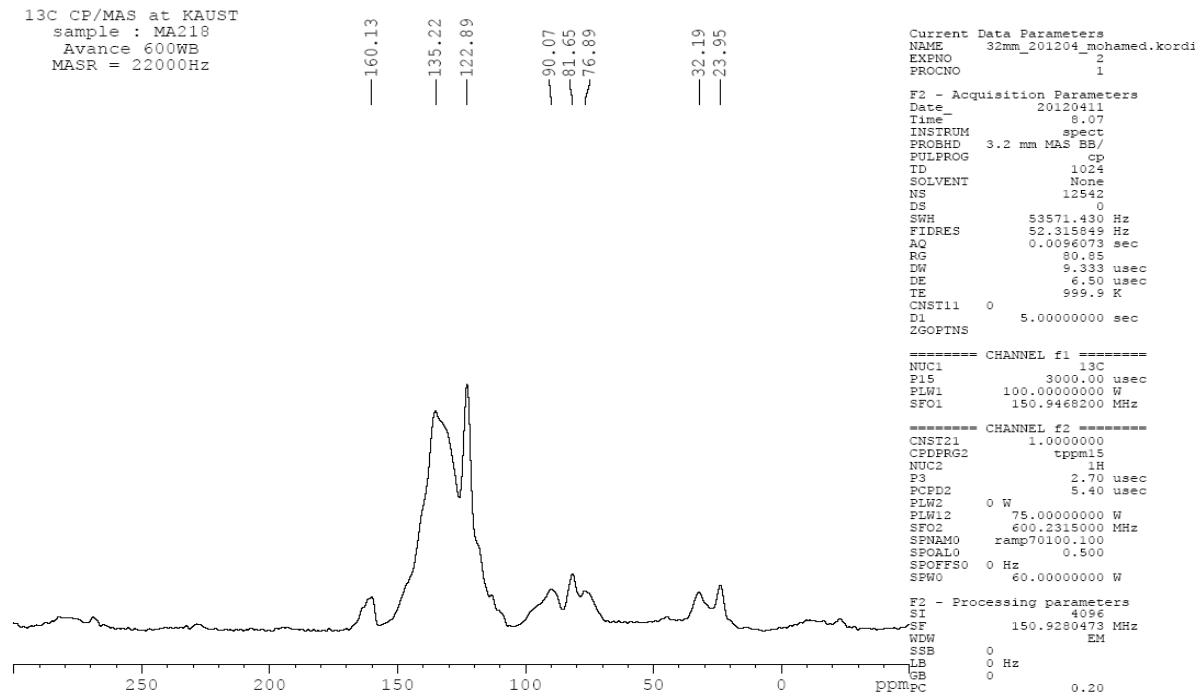


Figure S11. Solid-state CP-MAS NMR spectrum of 1

Scanning Electron Microscope (SEM) images of 1, 1-Cr and 1-Co

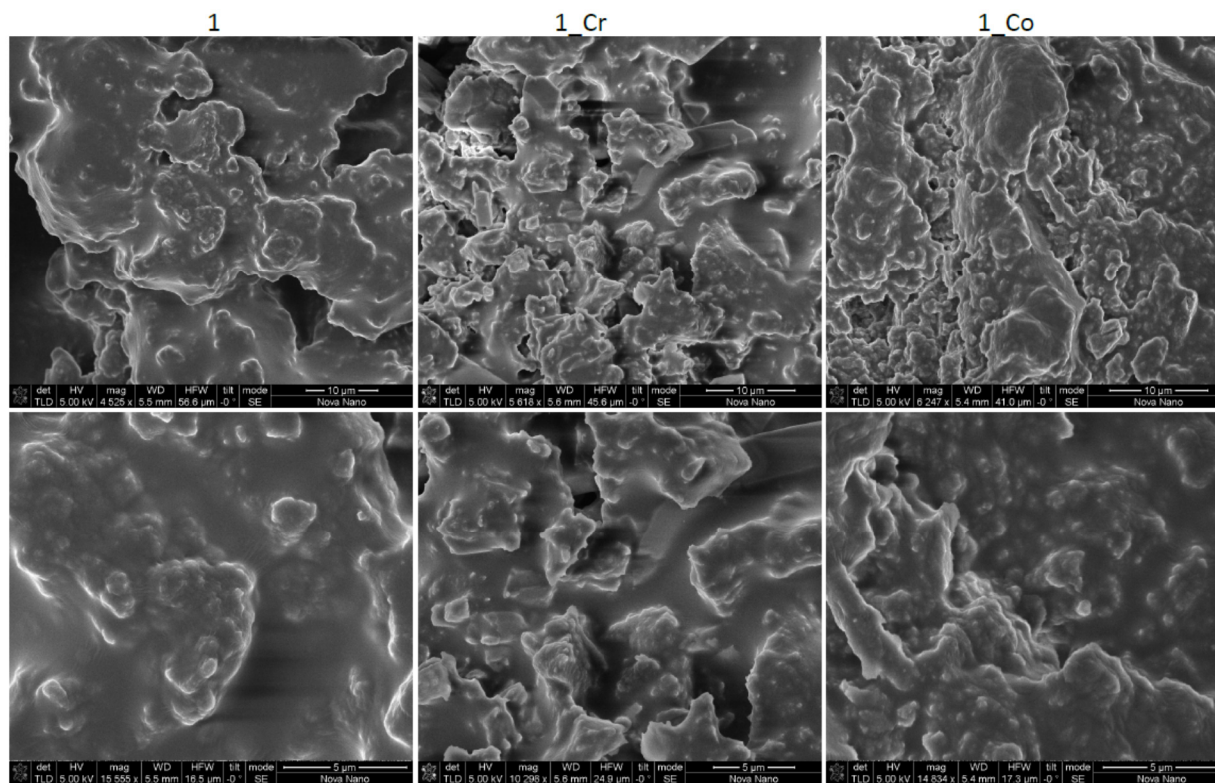
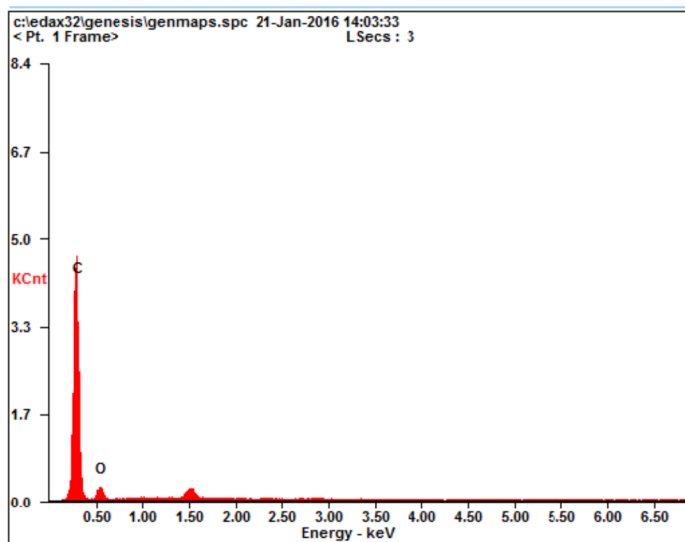


Figure S12. Scanning Electron Microscope (SEM) images of 1, 1-Cr and 1-Co

EDX (Energy-dispersive X-ray spectroscopy) analysis of 1, 1-Cr and 1-Co



<i>Element</i>	<i>Wt%</i>	<i>At%</i>
<i>CK</i>	84.20	87.66
<i>OK</i>	15.80	12.34
<i>Matrix</i>	Correction	ZAF

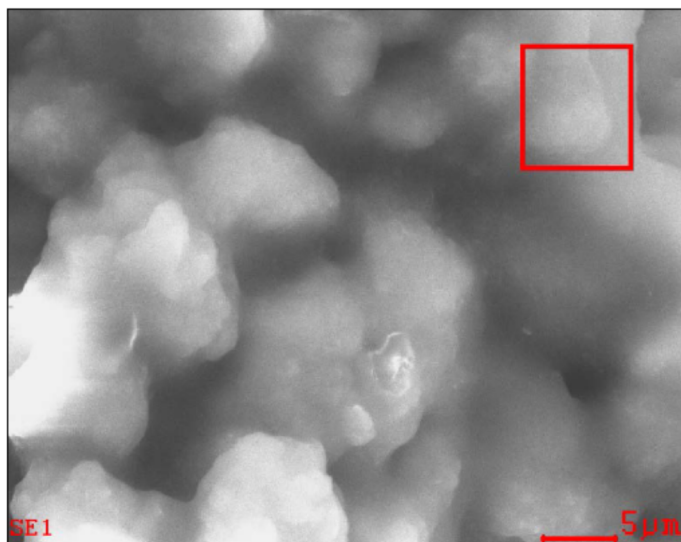
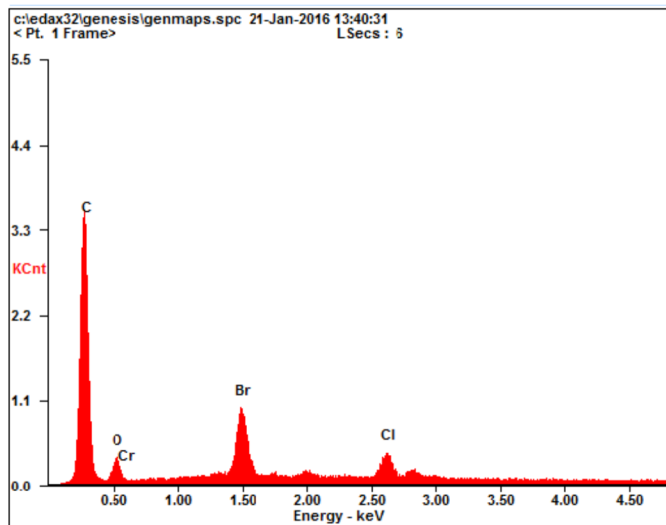


Figure S13. EDX analysis of 1



<i>Element</i>	<i>Wt%</i>	<i>At%</i>
<i>CK</i>	76.92	89.00
<i>OK</i>	08.47	07.36
<i>ClK</i>	02.19	00.86
<i>CrK</i>	06.72	01.80
<i>BrK</i>	05.70	00.99
<i>Matrix</i>	Correction	ZAF

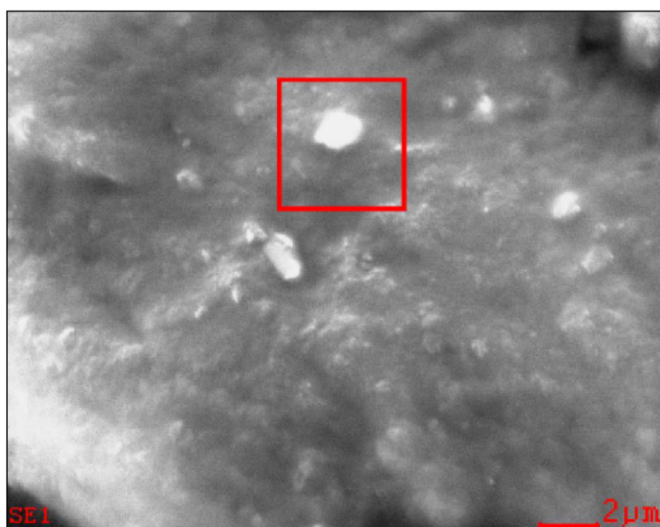
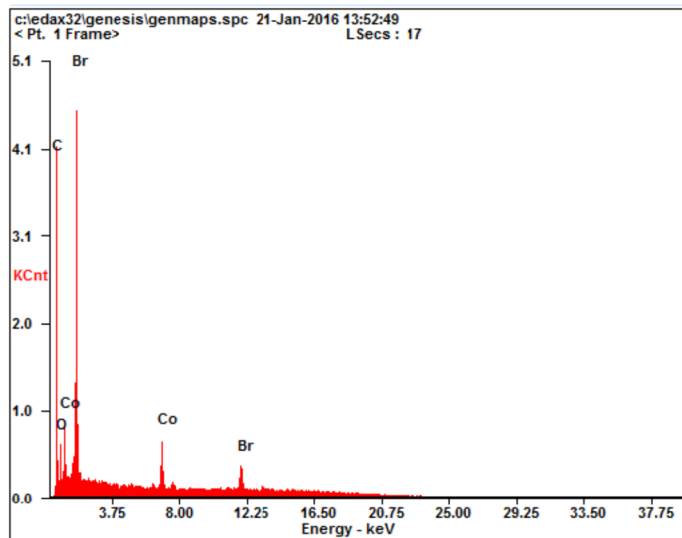


Figure S14. EDX analysis of 1-Cr



<i>Element</i>	<i>Wt%</i>	<i>At%</i>
<i>CK</i>	63.05	84.89
<i>OK</i>	08.85	08.95
<i>CoK</i>	06.68	01.83
<i>BrK</i>	21.42	04.33
<i>Matrix</i>	Correction	ZAF

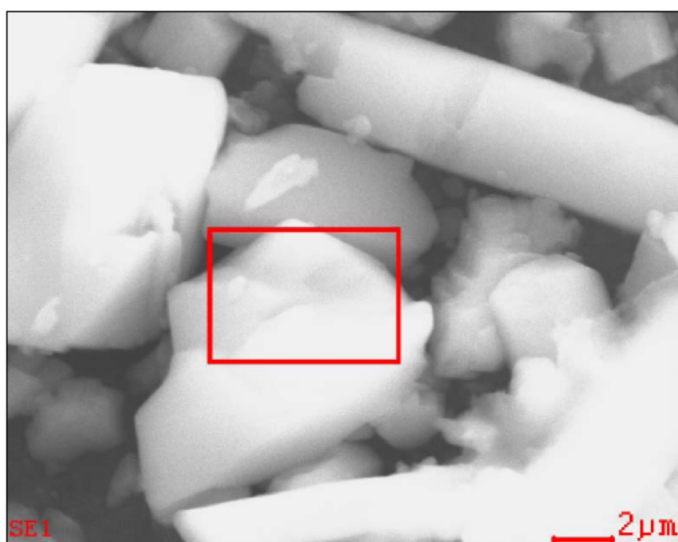


Figure S15. EDX analysis of **1-Co**

References

1. A. R. Silva, T. Mourão and J. Rocha, *Catalysis Today*, **2013**, 81.
2. V. Guillerm, Ł. J. Weseliński, M. H. Alkordi, M. I. H. Mohideen, Y. Belmabkhout, A. J. Cairns and M. Eddaoudi, *Chem. Commun.* **2014**, 50, 1937.
3. (a) I. Grohmann, E. Kemnitz, A Lippitz and W. E. S. Unger, *Surf. Interface Anal.*, **1995**, 23, 887; (b) T. Gross, D. Treu, E. Ünveren, E. Kemnitz and W. E. S. Unger, *Surf. Sci. Spectra*, **2008**, 15, 77; (c) M. Aronniemi, J. Sainio and J. Lahtinen, *Surf. Sci.*, **2005**, 578, 108.
4. (a) T.J. Chuang, C.R. Bridle and D.W. Rice, *Surf. Sci.*, **1976**, 59, 413; (b) C. A. F. Vaz, D. Prabhakaran, E. I. Altman and V. E. Henrich, *Phys. Rev. B*, **2009**, 80, 155457.